



Enhanced dispersion and stability of gold nanoparticles on stoichiometric and reduced TiO₂(1 1 0) surface in the presence of molybdenum

László Bugyi, András Berkó, László Óvári, Anna M. Kiss, János Kiss *

Reaction Kinetics Research Laboratory, Chemical Research Centre of the Hungarian Academy of Sciences, University of Szeged, P.O. Box 168, H-6701 Szeged, Hungary

ARTICLE INFO

Article history:

Received 16 October 2007

Accepted for publication 25 February 2008

Available online 4 March 2008

Keywords:

Oxygen-deficient

TiO₂(1 1 0) surface

Mo

Au

Nanoparticles

Bimetallic system

Enhanced dispersion

Thermal stability

ABSTRACT

Mo, Au and their coadsorbed layers were produced on nearly stoichiometric and oxygen-deficient titania surfaces by physical vapor deposition (PVD) and characterized by low energy ion scattering (LEIS), X-ray photoelectron spectroscopy (XPS), Auger electron spectroscopy (AES) and scanning tunnelling microscopy (STM). The behavior of Au/Mo bimetallic layers was studied at different relative metal coverages and sample temperatures.

STM data indicated clearly that the deposition of Au on the Mo-covered stoichiometric TiO₂(1 1 0) surface results in an enhanced dispersion of gold at 300 K. The mean size of the Au nanoparticles formed at 300 K on the Mo-covered TiO₂(1 1 0) was significantly less than on the Mo-free titania surface (2 ± 0.5 nm and 4 ± 1 nm, respectively). Interestingly, the deposition of Mo at 300 K onto the stoichiometric TiO₂(1 1 0) surface covered by Au nanoparticles of 3–4 nm (0.5 ML) also resulted in an increased dispersity of gold. The driving force for the enhanced wetting at 300 K is that the Au–Mo bond energy is larger than the Au–Au bond energy in 3D gold particles formed on stoichiometric titania. In contrast, 2D gold nanoparticles produced on ion-sputtered titania were not disrupted in the presence of Mo at 300 K, indicating a considerable kinetic hindrance for breaking of the strong Au–TiO_x bond.

The annealing of the coadsorbed layer formed on a strongly reduced surface to 740 K did not cause a decrease in the wetting of titania surface by gold. The preserved dispersion of Au at higher temperatures is attributed to the presence of the oxygen-deficient sites of titania, which were retained through the reaction of molybdenum with the substrate. Our results suggest that using a Mo-load to titania, Au nanoparticles can be produced with high dispersion and high thermal stability, which offers the fabrication of an effective Au catalyst.

© 2008 Elsevier B.V. All rights reserved.

1. Introduction

The formation of metal nanoparticles on different oxide supports is of great technological importance in catalysis, gas-sensing and materials science. TiO₂ has excellent properties as a support material, and it may change the catalytic activity of the supported particles in an advantageous way. It has been emphasized that the electronic interaction with the supported catalyst particles has an important role in determining the effect of semiconductor supports, like titania [1] and the electrical contribution to the so-called strong metal-support interaction was also established [2]. The effect of boundary lines between the catalyst and the support was also suggested [1]. It is frequently emphasized that in the wetting of titania, the reactivity of the overlayer metal towards oxygen is one of the decisive factors [3]. On the other hand, it was confirmed that the reducibility of an oxide support is in good correlation with the activation of oxygen molecules on oxygen vacancies of the support [4].

The present study was initiated by the observation that Au showing bilayer structure and complete wetting of epitaxial TiO_x/Mo(1 1 2) surface has an outstanding catalytic performance in the low temperature CO + O₂ reaction [5,6]. The surface composition of this adlayer was found Ti₂O₃, containing Ti³⁺ surface sites [7]. The role of an ultrathin reducible oxide support in the activity of catalytic metal nanoparticles has also been addressed in an earlier work [8]. It was concluded that the “dynamic interface fluxionality”, i.e. the ability of atoms to rearrange at the metal-oxide interface during adsorption may play an active role in the reaction. In the present article the possible influence of molybdenum on the wetting behaviour of Au deposited onto stoichiometric and oxygen-deficient TiO₂ surface is studied. Note that we formed Mo and Au nanoparticles on titania, what is different in several aspects from the case when the Mo atoms of a single crystal are present in the subsurface position of a supported titania layer [6].

Considering the complexity of the titania/gold/molybdenum system, we give a brief account of the interactions between the constituents of this material combination. The growth of gold

* Corresponding author. Tel.: +36 62 544 803; fax: +36 62 420 678.

E-mail address: jkiss@chem.u-szeged.hu (J. Kiss).

nanoparticles on stoichiometric $\text{TiO}_2(1\ 1\ 0)$ surface was thoroughly studied by LEIS, XPS and LEED methods [9]. It was concluded that Au initially grows in the form of 2D-like islands at 300 K on $\text{TiO}_2(1\ 1\ 0)$ without any significant chemical interaction with the support. Moreover, there was not any indication of the encapsulation of Au up to 775 K. In contrast to this, a rather complex charge transfer behaviour was deduced for Au supported on stoichiometric and oxygen-deficient TiO_2 surfaces by Okazawa et al. [10]. The effect of the reduction of the surface on the growth of gold nanoparticles on $\text{TiO}_2(1\ 1\ 0)$ was examined in an earlier STM work [11]. It was experienced that Au deposition on argon-ion sputtered titania resulted in a more dispersed Au overlayer at 300 K than on the stoichiometric oxide.

The separate deposition of gold and molybdenum on a $\text{TiO}_2(1\ 1\ 0)-(1 \times 2)$ reconstructed surface was already characterized by STM [11,12]. It was found that Au nanoparticles suffered considerable sintering at 700 K, whereas Mo nanoparticles showed remarkable resistance to sintering under the same circumstances. The difference was interpreted in terms of a stronger interaction between Mo and the TiO_2 , attributable to a partial oxidation of molybdenum at the interface. The oxidation of the molybdenum layers was accompanied by the reduction of TiO_2 already during the deposition performed at 300 K [13].

Regarding the above studies, it seems also relevant to consider the wetting of the titania surface by different molybdenum oxides. It was reported earlier that the deposited MoO_3 first spread out on the TiO_2 surface on the effect of annealing at 723 K, which was followed by the formation of surface polymolybdate compound at higher temperatures in the presence of water vapor [14]. At the same time, it was found by STM that the bonding of gold with oxidized molybdenum was weaker than with oxygen-deficient titania [15]. The wetting behaviour between gold and molybdenum oxides was also studied and it was found that an oxidation treatment led to the spreading out of Mo nanoparticles on the $\text{Au}(1\ 1\ 1)$ plane [16]. This latter observation suggests that the oxidation of molybdenum may also play a role in the wetting of Mo-covered titania by gold. It is worth noting that the thermally induced wetting may occur on an inert oxide, see for example the wetting of silica by Pt explained by an interfacial mixing between Pt and SiO_2 [17].

The study of the interaction between molybdenum and $\text{Au}(1\ 1\ 1)$ single crystal led to the conclusion that although the two metals are immiscible in the bulk phase [18], they can form a so-called surface alloy [19]. Mo nanoparticles formed through physical vapor deposition (PVD) was found to be encapsulated by gold after thermal activation, what was explained with the lower surface energy of Au compared to that of Mo [20]. In the study of the electronic interaction between $\text{Mo}(1\ 1\ 0)$ crystal plane and Au atoms, it was found that molybdenum induced a decrease in the population of Au 5d electron orbital [21]. In the case of Au layers grown on $\text{Mo}(1\ 1\ 1)$ surface, a layer by layer growth mode was experienced at 300 K, although the annealing at higher temperatures resulted in a preferential decoration of terrace edges [22].

In the present work, LEIS, XPS and STM measurements are presented to reveal structural information on the Au and Mo mono- and bimetallic ultrathin layers grown on titania surfaces. The results prove that the combined application of the above methods can largely contribute to a deeper insight into the atomic scale structure of the bimetallic systems.

2. Experimental

The experiments were performed in two separate ultrahigh vacuum (UHV) systems (base pressure $<5 \times 10^{-8}$ Pa). The first one was equipped with facilities for LEIS, AES, and XPS measurements (pre-

viously described in [23–26]), in the second one STM and AES techniques were used. Two similar $\text{TiO}_2(1\ 1\ 0)$ samples were cleaned and exposed to Au and Mo in the same way in the two UHV chambers. In this way, the samples were not transferred between them. Special attention was paid to the cross-calibration of the Au and Mo coverages (see below). LEIS spectra were obtained using the same Leybold EA10/100 hemispherical analyzer as for XPS and AES but with the polarity of the voltage biases inverted to detect He^+ ions. For all methods, spectra were collected at 300 K sample temperature. AES was performed with 2.5 keV primary electron energy and 5 V modulation. XPS measurements were carried out with a constant 100 eV pass energy, at a take-off angle of 17° (with respect to surface normal) using an Al $K\alpha$ X-ray anode. The binding energy scale was referenced to the position of the $\text{Ti}2p$ emission for the stoichiometric clean oxide, set to 459.0 eV [9,13,26,32]. XP peaks were fitted using Gauss–Lorentz functions, after background subtraction (Shirley). The relative area of peaks in the $\text{Ti}2p$ doublet was set to 2:1. In the measurements the binding energy range of 450–470 eV were used for the $\text{Ti}2p$ region. In this way the X-ray satellites and the satellite structure at higher energies [27,28] was not considered. Separate test measurements were performed, however, for a wider energy range at two extreme states of the surface (nearly stoichiometric and sputtered TiO_2), followed by a fitting taking also into account the satellite features. Based on this we can state that the error, introduced by the narrower energy regime in the determination of the composition of the sample, as regards the Ti oxidation states, is less than 5%. Our conclusions in this paper are based on much higher differences. The same approach for the fitting of the $\text{Ti}2p$ region is frequently used [13]. It is known from literature data that TiO is metallic, leading to a Doniach–Šunjić lineshape of $\text{Ti}2p$ [29]. For this reason asymmetry for the Ti^{2+} components was allowed, which did not result, however, in any improvement in the fitting in our case.

A Specs IQE 12/38 ion source was used for LEIS. He^+ ions of 800 eV kinetic energy were used at an ion flux equal to $0.03\ \mu\text{A}/\text{cm}^2$, what was necessary to avoid the sputtering of Au-containing surfaces. The incident angle (with respect to surface normal) was 50° , while the scattering angle was 95° . Areas of peaks due to He^+ ions scattered in single collisions were used to calculate LEIS peak ratios [25,26]. The error bars in the figures represent the standard deviation about the mean data value. Typically less than $\pm 5\%$ scattering was experienced about the mean value for LEIS data. The STM measurements were carried out by a commercial room temperature STM head (WA-Technology). The pictures of 256×256 pixels were recorded with the bias of +1.5 V (on the sample) and of 0.05 nA tunnelling current with an electrochemically etched W-tip. The images were scanned within 3 min on average [30]. Regarding the local nature of STM measurements, special attention was paid to the uniformity of the detected features over macroscopic distances (few mm-s) on the sample surface.

The $\text{TiO}_2(1\ 1\ 0)$ single crystals were products of PI-KEM. The samples were attached to a Ta plate with an oxide glue (AREMCO, ceramobond 571), and could be heated with a W filament placed behind the Ta plate. The sample temperature was measured by a chromel–alumel thermocouple, attached to the side of the sample with the same adhesive material. The heating and cooling rates during cleaning and all measurements presented here were always less than 2 K/s, regulated by a computer-controlled circuit.

An EGN4 e-beam evaporator of Oxford Applied Research was used for the deposition of Mo and Au. The amount of the deposited metals is expressed in equivalent monolayers (ML): 1 ML is defined as the amount of metal, arranged in the close-packed structure ((111) for gold and (110) for molybdenum) required to cover the substrate with a single atomic layer. This definition is frequently used in the literature [9,36]. The surface concentrations of the deposited metals in the STM chamber were estimated from

the volume of the nanoparticles (after a short annealing at 500 K for Au and at 900 K for Mo) [11,31]. In the XPS-LEIS chamber the coverage of gold was determined both by XPS and LEIS. In XPS, Ti2p, O1s and Au4f peak/doublet areas measured before and after deposition were used to obtain the gold surface concentration. An island-on-plane model was assumed, using the photoelectric cross-sections of Scofield [41], and inelastic mean free paths (IMFP) obtained from the TPP-2M equations [42]. The IMFP's in titania for Ti2p and O1s photoelectrons were 2.17 and 2.04 nm, respectively. The IMFP's in gold for Au4f, Ti2p, and O1s electrons were 1.58, 1.26, and 1.19 nm, respectively. At small coverages gold forms two-dimensional clusters on titania (see below), with a thickness of one atomic layer. In this range the Ti LEIS signal decrease, as a function of the evaporation time is proportional to the coverage and extrapolating the Ti signal decrease to zero intensity gives the 1 ML. Calibration of the gold surface concentration by LEIS and XPS showed reasonable agreement (with an accuracy of 25%). We preferred the coverage scale obtained from LEIS, because in the calculations based on the XPS data external parameters (cross-sections, IMFP's) also had to be used. In the case of Mo, the AES peak-to-peak intensity ratio ($\text{Mo}_{186\text{ eV}}/\text{Ti}_{385\text{ eV}}$) was applied to fit the coverage data in the two separate UHV systems. All depositions of the metals were performed at 300 K. The deposition rate was typically in the range of approximately $0.1\text{--}0.3\text{ ML min}^{-1}$ for both metals.

The typical cleaning procedure of titania consisted of Ne^+ ion bombardment (2 keV , $3 \times 10^{-6}\text{ A cm}^{-2}$, 300 K, 2 h) and annealing at 900 K. It is known from our previous STM investigations that similar treatments result basically in (1×1) bulk terminated registry, although the presence of 1–2% of defect sites (0D dots and 1D strings of Ti_2O_3 stoichiometry) cannot be excluded [31,32]. The long range ordered (1×2) reconstruction of $\text{TiO}_2(110)$ surface does not occur at these relatively low temperatures. The contamination level was kept below the detection limit of AES.

It is well known that ion bombardment causes a preferential sputtering of the surface oxygen. As a result, the surface of titania becomes oxygen-deficient. It was found by LEIS and XPS that a slightly oxygen-deficient surface could be oxidized even at 300 K by the adsorption of O_2 , but the strongly oxygen-deficient surface (prepared by Ar^+ ion bombardment) could be completely reoxidized only at higher temperatures [33,34]. The latter behaviour was attributed to the presence of subsurface defect sites. As the reduction of titania with Ar^+ ion sputtering resulted in a higher stability of the supported gold nanoparticles [11], in some experiments Au was deposited on oxygen-deficient surfaces formed with Ne^+ ion bombardment. Regarding that LEIS is sensitive only to the topmost surface layer, the elemental peak ratios can be related to the surface stoichiometry [35]. The nearly stoichiometric TiO_2 produced by annealing at 1000 K was reproducibly characterized by an O/Ti ratio of 0.70–0.85. This sample had the electrical conductivity suitable for spectroscopic measurements. Strongly oxygen-deficient surfaces were produced through in this work by neon- or argon-ion sputtering; the lowest O/Ti LEIS ratio was 0.45–0.50. A thorough ion-bombardment of titania resulted reproducibly in a surface with a given O/Ti LEIS peak height ratio both in our case and in a former study [33].

3. Results and discussion

3.1. Deposition of Au on $\text{TiO}_2(110)$ surface

A detailed scanning tunnelling microscopy study of Au deposited on clean and Ar^+ ion bombarded $\text{TiO}_2(110)$ surface can be found in our previous paper [11]. On the clean $\text{TiO}_2(110)$ surface the average diameter of Au particles is 4.3 nm at approximately

monolayer coverage of gold. The mean size of the gold particles changed only slightly upon the thermal treatment (up to 700 K). In the present chapter the experimental results obtained mainly by LEIS method will be presented and analyzed. The main conclusions match quite well to former STM results.

The observation that the Au LEIS signal increased linearly and Ti signal decayed also linearly at the lowest deposition times of Au on the nearly stoichiometric titania surface at 300 K (Fig. 1A) is in harmony with an earlier suggestion for 2D-like initial growth of Au nanoparticles on TiO_2 up to 0.15 ML coverage [9]. The 3D growth of Au particles above this coverage is manifested by deviation from linearity. Note that in harmony with former observation [9], we have also detected that a large part of titania is uncovered even at 4–5 ML equivalent gold coverages. At higher O-deficiency, the breakpoint in LEIS signals and the corresponding coverages shift to higher values as it was observed in a former study [36]. It was presented in that work that due to Ar^+ -ion sputtering of titania the critical Au-coverage for 2D growth increased up to 0.25 ML. The O/Ti LEIS ratio slightly increased as a result of gold deposition on a stoichiometric surface (not shown). The deposition of Au (0.70 ML) on the heavily ion-sputtered titania ($\text{O/Ti} = 0.45\text{--}0.50$) resulted in the increase of the O/Ti ratio to the value characteristic for the stoichiometric surface (0.7–0.85, see first point in Fig. 1B). The increase of the O/Ti ratio after Au deposition both on nearly stoichiometric and heavily sputtered surfaces can be related to the bonding of Au to the reduced centers of titania, where the coor-

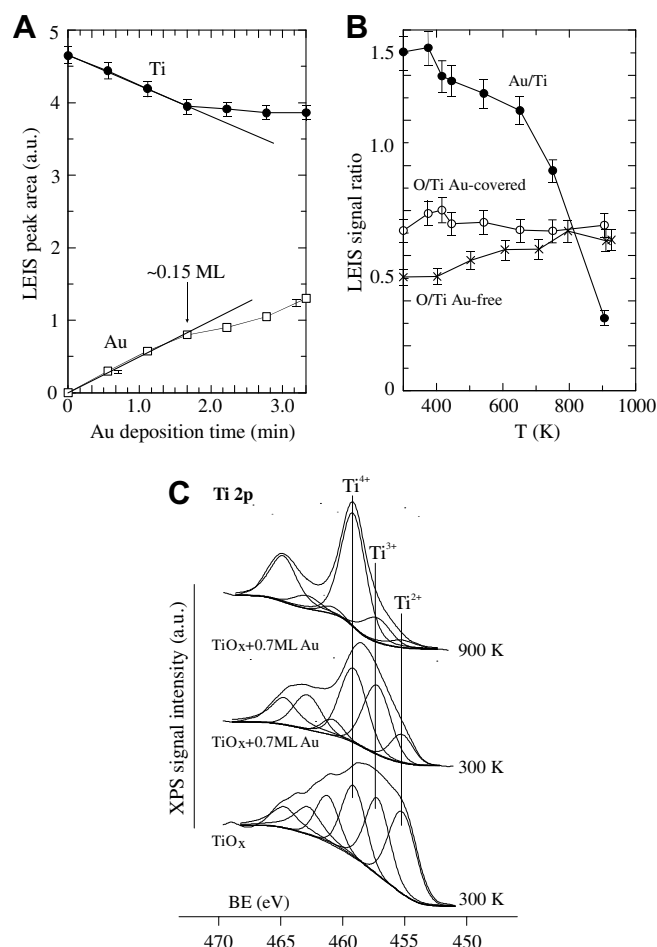


Fig. 1. (A) Change of LEIS peak area of Au and Ti as a function of Au deposition time at low coverages (stoichiometric surface). The effect of thermal treatments for an Au-free and Au-covered, Ne^+ sputtered surface (B) on the O/Ti and Au/Ti LEIS ratios ($\theta_{\text{Au}} = 0.70\text{ ML}$) and (C) on the Ti2p XPS signals ($\theta_{\text{Au}} = 0.70\text{ ML}$).

dination of Au atoms is the highest, leading to a more efficient shadowing of Ti sites by the gold clusters.

Since on a reduced sample, both higher dispersity and thermal stability of gold nanoparticles can be achieved [11], the thermal stability of gold nanoparticles formed on an oxygen-deficient surface (produced by Ne⁺ ion sputtering, 20 min, 1 μ A, 2 keV) was followed by LEIS and XPS (Fig. 1B and C). The heating of the Au-covered (0.70 ML) surface to 650 K led to a decrease in the relative Au LEIS signal which can be attributed to moderate sintering. Above 650 K, the Au signal decreases steeply, indicating a marked Au particle aggregation. Beside sintering, the onset of the evaporation of supported gold particles may also contribute to the decrease in Au LEIS signals after annealing to 900 K. This conclusion is in harmony with our earlier STM measurements [11]. Note that the O/Ti ratio remained essentially unchanged during the heat treatments, suggesting that the composition of uncovered titania remained constant. For comparison, the O/Ti ratio for the Au-free surface is also plotted in Fig. 1B. In contrast to the observation for the Au-covered surface, the enhancement of this ratio to 0.70 at 800 K indicates that the surface concentration of oxygen on the Au-free titania increased. The extent of change in the O/Ti ratio with temperature is similar to that observed with other methods [37].

The XP spectrum of titania sputtered by Ne⁺ ions is presented in Fig. 1C. By fitting of the appropriate peaks it is shown that this strongly perturbed titania surface contains Ti⁴⁺, Ti³⁺ and Ti²⁺ ions in nearly equal amounts. After the deposition of 0.70 ML gold at 300 K, the relative abundance of Ti²⁺ ions decreases, suggesting some electron transfer from oxygen vacancy sites onto the gold nanoparticles. Note that the deposition of Au onto reduced titania surface caused the oxidation of Ti³⁺ ions to Ti⁴⁺ ions [5] and similarly, the deposition of Rh onto Ar-ion bombarded titania, the reduced Ti³⁺ state was oxidized back to Ti⁴⁺ state [32]. The positions of the Ti³⁺ and Ti²⁺ peaks agrees well with literature data [38]. After annealing to 900 K, the contribution of Ti³⁺ and Ti²⁺ signals to the Ti2p signal is reduced to 24%. The oxidation process of surface can be attributed either to the diffusion of oxygen from the bulk of titania into the surface regions or to the migration of Ti ions into the bulk [37]. Since a stoichiometric titania surface is weakly wetted by gold [36], the heat treatments resulting in the strong oxidation of surface necessarily causes the sintering of gold particles.

3.2. Deposition of Mo on TiO₂(110) surface

The deposition of molybdenum onto a Ne⁺-ion sputtered titania surface was performed at 300 K. LEIS spectra for the Mo-free and Mo-covered samples are presented in Fig. 2A. From the initial linear change in the Ti signal we may conclude that the PVD of Mo resulted in highly dispersed deposit and in the formation of 2D-like particles (Fig. 2B). This seems to be in harmony with former observations. A 2D-like growth of particles was observed earlier by STM on a stoichiometric titania [31]. A Stranski–Krastanov type growth was established by AES for either stoichiometric or reduced titania [13], corresponding to the completion of first molybdenum layer before developing the second one. In our case, at the highest applied Mo-coverage the O/Ti LEIS ratio reached ~ 1.0 . Since this value is higher than that characteristic for the stoichiometric titania, it indicates the reaction of oxygen with Mo particles. The background gas may also contribute to this effect. The strong decrease in the Ti-signal in Fig. 2B at the initial Mo-deposition reflects the high affinity of Mo towards the titanium centers of titania, where its coordination to O atoms is the highest.

Due to the great chemical reactivity of Mo-particles formed on both stoichiometric and reduced titania surfaces towards oxygen, only the change in Ti LEIS signals was analysed to follow the sinter-

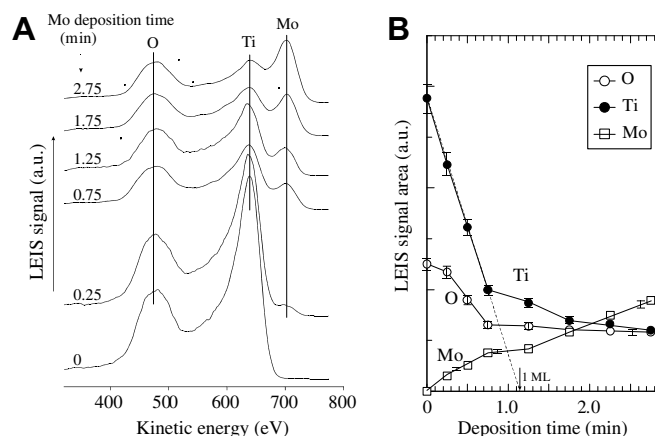


Fig. 2. (A) LEIS signals of a reduced titania surface covered by different amounts of molybdenum and (B) the corresponding change of Mo, Ti and O LEIS peak areas.

ing of Mo-particles during thermal treatment of Mo-covered (1 ML) titania (not shown). According to a former observation [12], these signals indicated that sintering began at ~ 750 K. Above this temperature, the increase in Ti and O signals beside sintering may also indicate the partial encapsulation of Mo particles, which was suggested in a former study [31]. The nearly perfect encapsulation of Mo nanoparticles was really observed when the surface covered with 4.5 ML of Mo nanoparticles was bombarded by Ne⁺ ions (20 min, 2 keV, 1 μ A) during annealing the sample at 900 K. As it can be seen in Fig. 3, after this treatment the LEIS shows a very faint Mo LEIS signal (Fig. 3B), but a pronounced amount of Mo can be detected in the subsurface layers by AES (Fig. 3C). Taking into account the information depth of these methods, the titania overlayer is estimated to be 1–2 ML thick. XPS data indicate clearly that the titanium is present only in Ti⁴⁺ oxidation state after this treatment, i.e. it forms an essentially stoichiometric oxide in the ion-assisted encapsulation process. Since the thickness of the titania layer produced during the encapsulation is similar to that formed on the Mo(112) surface applied for supporting Au layers [5], it deserves a further detailed study.

3.3. Deposition of Mo on TiO₂(110) surface doped with Au

Since gold deposited on titania single crystal exhibits a great chemical and morphological stability at 300 K as it can be deduced from the above LEIS and former STM measurements [11], in the coadsorption experiments we first produced an Au layer and Mo was deposited onto it. The coadsorbed layers were formed on oxygen-deficient and stoichiometric surfaces as well. At low ($\theta_{\text{Au}} = 0.20$ ML) gold coverage, the deposition of Mo at 300 K on oxygen-deficient titania surface at and above 0.3 ML Mo coverage caused an approximately parallel decrease of LEIS signals characteristic of Ti, O and Au (Fig. 4A). This feature clearly indicates that these components are covered with nearly the same probability. Since the Mo–Au bond is stronger than the Mo–TiO_x bond [5], the bonding of Mo on top of the stable 2D Au particles is energetically favourable. The parallel decrease of Au and Ti signals suggests that the surface diffusion of Mo atoms is hindered.

At higher Au surface concentrations a different behaviour was observed. At around a coverage of $\theta_{\text{Au}} = 0.70$ ML, the deposition of 0.3 ML Mo on an oxygen-deficient surface caused negligible change in Au LEIS signal, indicating a moderate disruption of gold particles. Above this Mo-coverage a nearly parallel decrease was seen in the intensity of Ti, O and Au signals (Fig. 4B), indicating that Mo binds on top of Au, Ti and O sites. In Fig. 4C it is presented that the absolute LEIS intensity for gold (1 ML) intensifies considerably

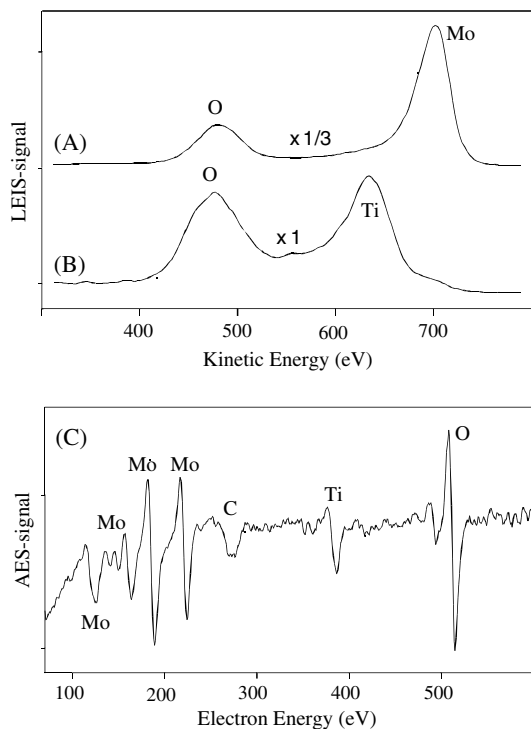


Fig. 3. (A) LEIS spectrum of freshly deposited (4.5 ML) Mo nanoparticles. (B) LEIS spectrum and (C) AES spectrum of molybdenum encapsulated by titania due to Ne^+ ion treatment (2 keV, 20 min, 900 K and $4 \times 10^{-6} \text{ A cm}^{-2}$).

with the deposition of Mo on stoichiometric titania. Note that after the exposure of 0.3 ML Mo to the stoichiometric surface, the absolute Au LEIS signal was intensified by about 20% even at high gold coverage of 2 ML. This surprising feature may be explained by an activated wetting of the surface by gold on the effect of Mo deposition. The question arises naturally what are the microscopic details of the Au LEIS peak intensity enhancement. One possible explanation could be the activated disruption of gold nanoparticles into smaller particles and another one is the flattening of the 3D Au nanoparticles. Since it was established in a former study that Au binds weaker even to the oxygen-deficient TiO_x film than to the Mo substrate [5], the increased dispersity can be related to the binding of gold to metallic Mo instead of TiO_x .

In order to observe the change in the morphology of the Au particles at room temperature on the effect of Mo deposition, STM measurements were made on stoichiometric samples prepared by similar treatments as in the case of the LEIS measurements. The STM image of $20 \text{ nm} \times 20 \text{ nm}$ in Fig. 5A shows the $\text{TiO}_2(110)$ surface after the deposition of 0.6 ML gold at RT. The Au nanoparticles exhibit a characteristic diameter of 3–4 nm and a height of 2–3 atomic layers. On the effect of the deposition of 0.25 ML of Mo the STM images indicate two characteristic changes (Fig. 5B): (i) although the number of the larger particles remains nearly the same, the size of these nanoparticles (probably gold) is significantly reduced (diameter of <2 nm, height of 1–2 atomic layers); (ii) besides this change, the surface is uniformly covered by new particles of much smaller average diameter (1 nm) which can be attributed to Mo– MoO_x nanoparticles containing some Au atoms [31]. The deposition of additional Mo (0.85 ML) at 300 K results in a general increase in the size of all particles, however, even the larger ones possess smaller diameter than that of the initial Au particles (Fig. 5C).

These STM data verify that Mo deposition results in the decrease of the Au particle size. In the light of the former LEIS measurements, however, gold is not removed from the surface. The

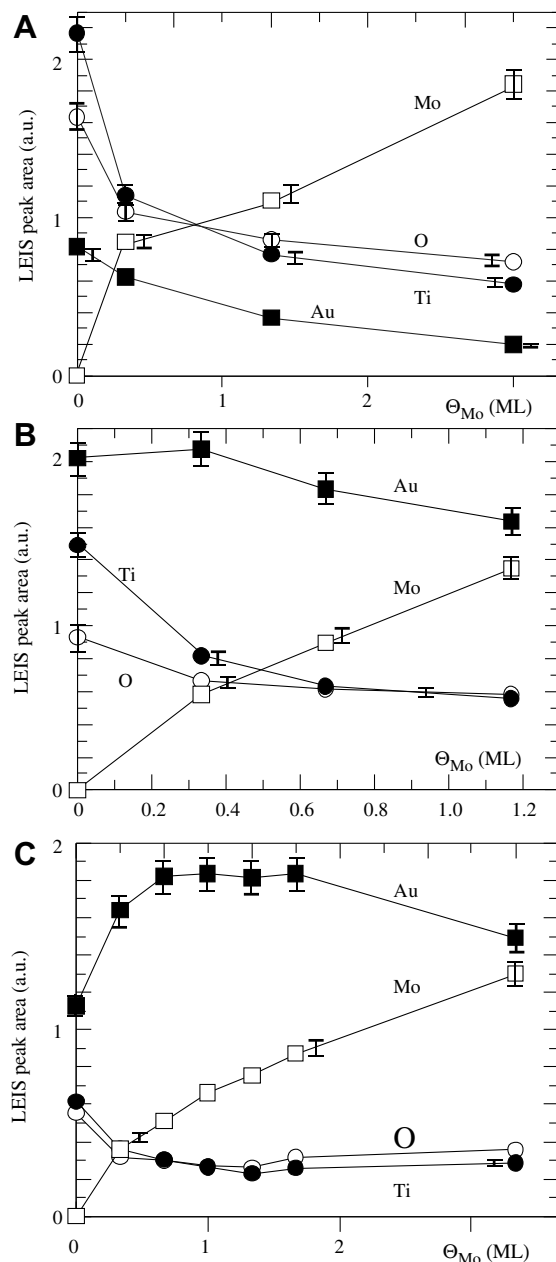


Fig. 4. Effects of Mo deposition on the Au, Mo, Ti and O LEIS peak areas on titania surfaces precovered by (A) 0.20 ML of gold (oxygen-deficient surface), (B) 0.70 ML of gold (oxygen-deficient surface) and (C) 1 ML of gold (stoichiometric surface).

common explanation of these LEIS and STM results can be made in terms of an enhanced mobility and activated detachment of gold atoms at the edge and corner positions of the Au particles on the effect of Mo deposition. It can be assumed that the diffusion of Au atoms of a nanoparticle is activated by the impinging Mo atoms due to different reasons: (i) the decrease in Au–Au bond strength owing to the formation of Mo–Au bond, resulting even in Mo–Au exchange and surface alloying [19], (ii) the reaction heat generated by the oxidation of Mo at the perimeter of Au nanoparticles. In terms of thermodynamic parameters it is well established that gold has lower surface free energy than molybdenum [20] and Au/Mo has larger binding energy than Au/ TiO_2 [5]. Although Mo is rather reactive and it is partially oxidized during the deposition by the O-content of titania [13], the adsorbing Mo atoms may cause structural changes in the deposited gold [20] and the wetting of

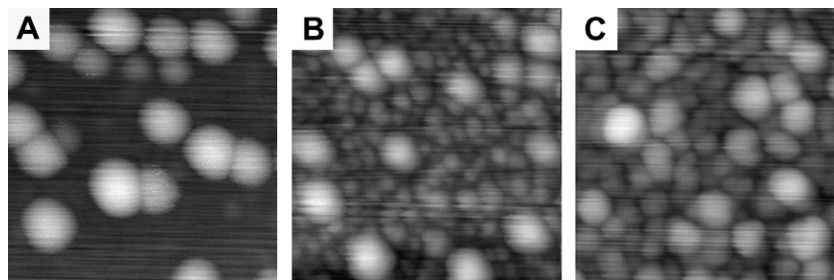


Fig. 5. Characteristic STM images ($20 \times 20 \text{ nm}^2$) recorded on a stoichiometric $\text{TiO}_2(1\ 1\ 0)$ surface pre-deposited by (A) 0.6 ML Au and the subsequent deposition of Mo (B) 0.25 ML and (C) 0.85 ML at room temperature.

oxidized and unoxidized molybdenum may occur [5,16,20]. In the case of low gold coverages where the formation of 2D particles on sputtered titania was also found by others [36], the Mo deposition caused a decrease in Au LEIS signals (Fig. 4A). It means that at 300 K the activation barrier for the disruption of 2D Au particles bonded to the reduced centers of titania is probably too high to be compensated by the adsorption energy of Mo either on titania or on gold [5].

Fig. 6 shows the change of the Au/Ti, Mo/Ti and O/Ti relative LEIS signals during stepwise annealing of stoichiometric and oxygen-deficient titania surfaces covered by Mo and Au. The annealing of a coadsorbed layer consisting of 2 ML Au and 0.4 ML Mo on a stoichiometric titania led to the LEIS intensity changes shown in Fig. 6A. The monotonous decrease in Au/Ti LEIS ratio is in accordance with the sintering of Au particles. It can be concluded that on stoichiometric titania a small amount of Mo cannot inhibit the sintering of Au.

In Fig. 6B the effect of annealing is presented on the Au/Ti, Mo/Ti and O/Ti relative LEIS signals of an oxygen-deficient titania surface precovered by 2 ML Au and post-deposited by 0.4 ML Mo. It is remarkable that the Au/Ti ratio is essentially unchanged up to 750 K. This observation is in harmony with a former finding that there is a strong interaction between gold and $\text{Mo}(1\ 1\ 2)/\text{TiO}_x$ surface, leading to its complete wetting by Au after thermal activation [5,6]. Since it was established that at higher temperatures MoO_x formed in the interfacial reaction between titania and Mo [38] and that there is a stronger interaction between TiO_x and gold than between Au and MoO_x [15], it is reasonable to assume that the increase in the stability of the Au/Ti LEIS ratio is caused in part by the migration of gold from oxidized molybdenum to the oxygen-deficient titania surface, i.e. the enhanced wetting of titania by gold.

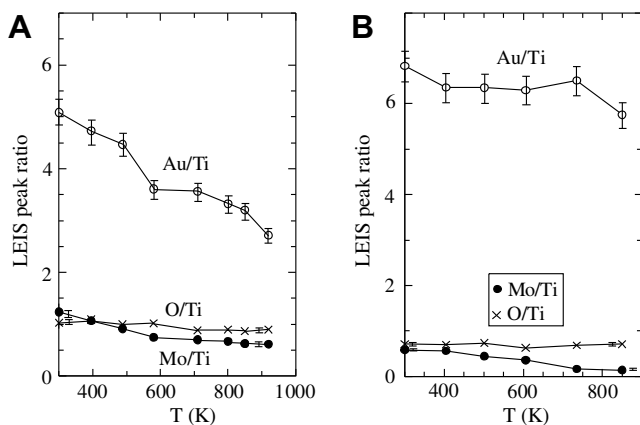


Fig. 6. Change of the relative LEIS peak intensity as a function of temperature: (A) 2 ML Au followed by deposition of 0.4 ML Mo (stoichiometric titania) and (B) 2 ML Au followed by 0.4 ML of Mo (reduced titania).

Above 750 K the Au/Ti ratio decreases, indicating the sintering of Au. The O/Ti ratio is essentially unchanged during thermal treatments, suggesting that the stoichiometry of uncovered part of titania surface has not changed. Note that the dissolution of oxygen atoms in Mo nanoparticles can make a part of oxygen undetectable by LEIS. The dissolution of O was also experienced on a $\text{Mo}(1\ 1\ 2)$

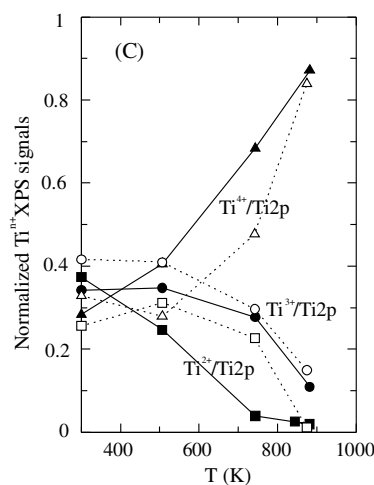
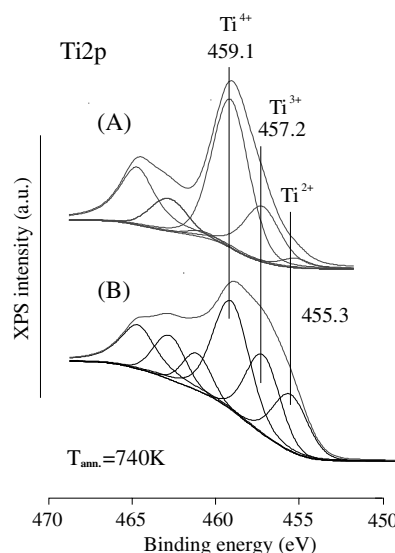


Fig. 7. Ti2p XPS spectra of (A) reduced titania surface and (B) reduced titania pre-deposited by 2 ML Au and post-deposited by 0.4 ML Mo, both after annealing to 740 K and (C) normalized Ti^{n+} XPS signal intensities as a function of temperature for the reduced titania surface and for the reduced titania pre-deposited by 2 ML Au, post-deposited by 0.4 ML Mo. Filled symbols refer to Ne^+ -ion sputtered titania, open symbols refer to $\text{TiO}_x + 2 \text{ ML Au} + 0.4 \text{ ML Mo}$ layer.

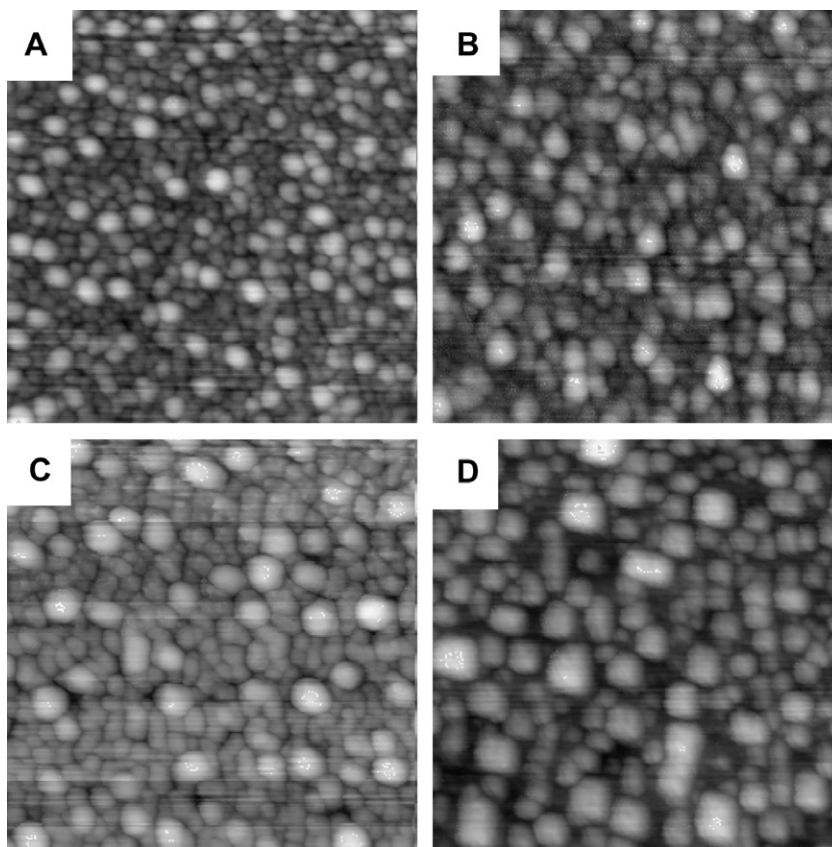


Fig. 8. STM images ($50 \times 50 \text{ nm}^2$) detected on the stoichiometric $\text{TiO}_2(1\ 1\ 0)$ surface (A) deposited by 0.6 ML of Au and post-deposited by 0.85 ML of Mo at 300 K and annealed subsequently at higher temperatures (B) 700 K, (C) 900 K and (D) 1000 K for 2 min in UHV.

surface for adsorbed oxygen at 800 K [39]. The slight decrease of Mo/Ti ratio in Fig 6A and B tentatively can be related to different phenomena: to structural rearrangements, to the oxidation of Mo or to its partial covering by Au.

In the case of the latter Au + Mo composition, the surface formed in the process described above was also studied by XPS (Fig. 7). As it can be seen from Fig. 7A, after annealing to 740 K, the contribution of Ti^{2+} line on the Mo-free surface is weak as compared with that of the $\text{TiO}_x/2 \text{ ML Au} + 0.4 \text{ ML Mo}$ layer (Fig. 7B). The summary of annealing experiment is shown in Fig 7C, where it is clearly presented that the $\text{Ti}2p$ line has a well detectable Ti^{2+} component for the $\text{TiO}_2/\text{Au} + \text{Mo}$ surface in a broad temperature-range of 500–800 K. The observation of a strongly reduced titania is in harmony with a former finding that in an ultrathin titania layer formed on $\text{Mo}(1\ 1\ 2)$ crystal Ti^{3+} ions remained unoxidized after annealing to 900 K [6] and allows to conclude that the reduced state of titania is crucial to attain an enhanced surface wetting by gold. The presence of Mo seems to be essential to reach a good wetting of titania at higher temperatures. The molybdenum at higher temperatures at least partly preserves the non-stoichiometric (oxygen-deficient) state of TiO_2 . Note that on longer time scale and at higher temperatures, the oxygen migrating to the surface from the bulk of titania single crystal oxidizes both the Mo nanoparticles and the oxygen-deficient titania surface, leading to the decrease in the wettability by gold. This might be avoided by applying an ultrathin titania overlayer, similarly to the method of Chen and Goodman [6].

In spite of the fact that the application of STM for the identification of the chemical composition of the nanostructures is rather difficult, in certain cases the morphological features can be clearly attributed to a special chemical component, for example on the ba-

sis of its surface concentration. The STM images ($50 \text{ nm} \times 50 \text{ nm}$) presented in Fig. 8 depict the effect of stepwise annealing on the nanomorphology of a stoichiometric TiO_2 sample predeposited by 0.6 ML of gold and post-deposited by 0.85 ML of Mo at 300 K (see also above in Fig. 5). Before the thermal treatments, the morphology of the surface exhibits well distinguished particles: (1) the larger ones correspond to the positions of the Au nanoparticles existing already before the deposition of Mo and probably decorated with some Mo atoms and (2) the smaller ones are basically consisting of Mo and MoO_x , however, some gold atoms are probably attached also to these particles (Fig. 8A). Note that although Mo and gold are immiscible in the bulk phase, the surface alloying on Mo nanoparticles may be favored, since nanoparticles are expected to be rich in surface vacancies and defects [40]. The annealing at 700 K in UHV for 2 min causes only a slight change in the surface morphology (Fig. 8B). In contrast to that, the annealing at 900 K results in a perceptible increase of the diameter of both particles, but actually they cover almost completely the empty regions of the support (Fig. 8C). Although it is difficult to differentiate between the particles of this STM picture, the increase in the diameter of largest particles on the initially stoichiometric titania surface suggests that a sintering of gold particles occurred, which is supported by the decrease of Au LEIS signal in Fig. 6A. We can assume that the more outriding particles with average diameter of 3–4 nm and height of 1.5–2.0 nm can be identified as gold or gold covered Mo sites. The presence of gold can affect the agglomeration of Mo by hindering its oxidation. On the effect of a further annealing at 1000 K (Fig. 8D), all the particles became more separated from each other showing an intensive agglomeration and evaporation of both gold and Mo (the latter one desorbs in the form of MoO_3 [31]).

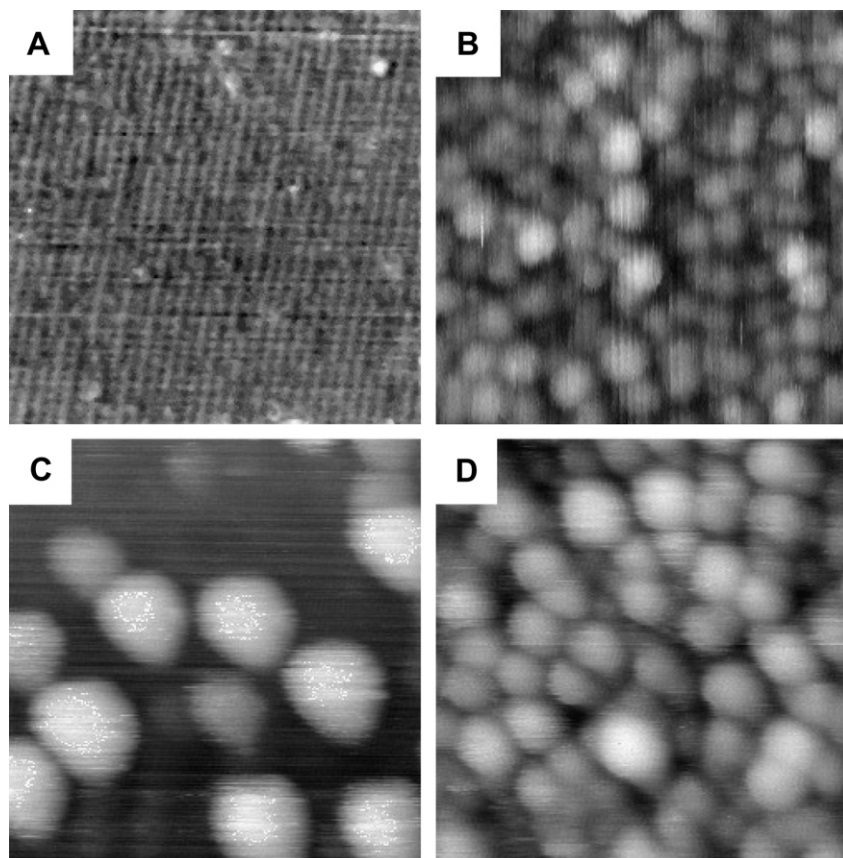


Fig. 9. STM images ($20 \times 20 \text{ nm}^2$) recorded (A) on clean $\text{TiO}_2(110)$ surface, on the support covered by monometallic deposition of (B) Mo (0.6 ML) and (C) Au (0.5 ML). The bimetallic surface can be seen on image (D) where the Mo (0.6 ML) covered surface was post-exposed to Au (0.5 ML) at 300 K.

3.4. Deposition of Au on $\text{TiO}_2(110)$ surface doped with Mo

In this series of experiments STM was applied to follow the morphological changes of a stoichiometric $\text{TiO}_2(110)$ surface covered by 0.6 ML of Mo and exposed to Au (0.5 ML). Fig. 9 shows the characteristic STM images ($20 \text{ nm} \times 20 \text{ nm}$) registered on surfaces of different compositions. Fig. 9A image depicts the 1×1 arranged $\text{TiO}_2(110)$ surface where the light rows running in the $[001]$ direction with an average distance of 6.5 nm can be attributed to Ti^{4+} atomic rows [31]. The deposition of 0.6 ML Mo onto this surface results in the formation of 1–1.5 nm sized round shape Mo– MoO_x nanoparticles (Fig. 9B). Much larger particles formed when 0.5 ML Au was deposited onto the clean $\text{TiO}_2(110)$ support at 300 K (Fig. 9C). The average diameter of these particles is 4–5 nm and the height is 0.7 nm. Totally different size distribution appears when the same amount of gold (0.5 ML) is deposited onto the above Mo precovered surface: the surface concentration of the particles is much higher (it is close to the number of Mo particles before Au deposition) and the size of the particles is smaller: diameter of 2.5 nm, height of 0.5 nm (Fig. 9D). This observation can be explained by the fact that Au bonds preferentially to metallic Mo and to the reduced centers of titania [5]. It is important to mention that because of the uncertainty of the imaging tip shape and the strong dependence of the recorded images on this parameter, several reproductions of these results were performed of nearly the same coverage and of different coverages, too. On the basis of different measurements, it was concluded that the surface coverages of Au and Mo used in Fig. 9 are optimal coverages to present the effect described above.

On the basis of the STM and LEIS measurements presented here for the Au/Mo bimetallic thin layers it can be concluded that the

presence of Mo in submonolayer coverages strongly affect the morphology of Au particles on stoichiometric titania both for the pre- and post-deposition of gold at 300 K. The main feature of the effect is the increased dispersity of Au particles.

4. Conclusions

The behaviour of Au/Mo bimetallic layers deposited on $\text{TiO}_2(110)$ depended on the surface stoichiometry of substrate, on the relative concentrations of the ad-metals and on the sample temperature.

- (i) In the case of a nearly stoichiometric titania, Mo deposition at 300 K caused a remarkable increase in the gold dispersity at larger Au coverages ($>0.6 \text{ ML}$), corresponding to the rupture of Au–Au bonds in 3D particles with low kinetic hindrance. The dispersion enhanced irrespective of the deposition sequence of the metals, what can be correlated to stronger Au–Mo and Au– TiO_x bond related to the Au–Au bond strength.
- (ii) On a strongly oxygen-deficient titania the disruption of 2D-like Au nanoparticles was not experienced after Mo deposition at 300 K. This is related to the strong bonding of these gold particles to TiO_x surface leading to a kinetic hindrance towards the rupture of Au–Au bond. At higher Au coverages, where 3D Au-clusters formed, Mo deposition resulted in a moderate disruption of Au particles, as indicated by LEIS.
- (iii) It was found in a broad range of coverages ($\theta_{\text{Au}} = 0.6\text{--}2 \text{ ML}$, $\theta_{\text{Mo}} = 0.25\text{--}0.85 \text{ ML}$) that annealing of the coadsorbed layers formed on the stoichiometric surface led to the sintering of

gold particles. This is attributed to the presence of stoichiometric titania and to the formation of oxidized Mo particles, which are not wetted well by Au.

- (iv) Heating up to 740 K the 2 ML Au + 0.4 ML Mo layer formed on a strongly reduced titania surface, the Au/Ti LEIS ratio remained unchanged, indicating that the dispersity of gold was preserved. At the same time, Ti remained partially in the form of Ti^{2+} , suggesting that the reduced state of titania plays a crucial role in the high dispersity and thermal stability of gold nanoparticles. The role of finely dispersed Mo is to react with the oxygen migrating out from the bulk of titania during thermal treatment and to keep the titania surface in reduced state.

In summary, the application of Mo-load results in an enhanced dispersity of gold nanoparticles on a nearly stoichiometric titania surface at 300 K and in a high thermal stability on the strongly reduced surfaces, offering the fabrication of more effective TiO_2 /Au catalysts.

Acknowledgements

This work was supported by grants OTKA (NI 69327, K 6920) and by grant NKFP 3A058-04 of the Ministry of Education. The authors thank gratefully the financial support by the Hungarian National Office of Research and Technology (NKTH) and the Agency for Research Fund Management and Research Exploitation (KPI) under Contract No. RET-07/2005.

References

- [1] F. Solymosi, *Catal. Rev.* 1 (1968) 233.
- [2] F. Solymosi, *J. Catal.* 94 (1985) 581.
- [3] U. Diebold, *Surf. Sci. Reports* 48 (2003) 53.
- [4] B. Grzybowska-Świerkosz, *Catal. Today* 112 (2006) 3.
- [5] M.S. Chen, K. Luo, D. Kumar, W.T. Wallace, C.-W. Yi, K.K. Gath, D.W. Goodman, *Surf. Sci.* 601 (2007) 632.
- [6] M.S. Chen, D.W. Goodman, *Science* 306 (2004) 252.
- [7] D. Kumar, M.S. Chen, D.W. Goodman, *Thin Solid Films* 515 (2006) 1475.
- [8] S.Y. Quek, C.M. Friend, E. Kaxiras, *Surf. Sci.* 600 (2006) 3388.
- [9] L. Zhang, R. Persaud, T.E. Madey, *Phys. Rev. B* 56 (1997) 10549.
- [10] T. Okazawa, M. Kohayama, Y. Kido, *Surf. Sci.* 600 (2006) 4430.
- [11] A.M. Kiss, M. Svec, A. Berkó, *Surf. Sci.* 600 (2006) 3352.
- [12] J.R. Kitchin, M.A. Barteau, J.G. Chen, *Surf. Sci.* 526 (2003) 323.
- [13] B. Domenichini, S. Pétigny, V. Blondeau-Patissier, A. Steinbrunn, S. Bourgeois, *Surf. Sci.* 468 (2000) 192. and references therein.
- [14] R. Margraf, J. Leyer, H. Knotzinger, E. Taglauer, *Surf. Sci.* 189/190 (1987) 842.
- [15] C. Xu, W.S. Oh, G. Liu, D.Y. Kim, D.W. Goodman, *J. Vac. Sci. Technol. A* 15 (1997) 1261.
- [16] Z. Song, T. Cai, J.A. Rodriguez, J. Hrbek, A.S.Y. Chan, C.M. Friend, *J. Phys. Chem.* 107 (2003) 1036.
- [17] R. You, H. Song, X.-F. Zhang, P. Yang, *J. Phys. Chem. B* 109 (2005) 6940.
- [18] C.T. Campbell, *Annu. Rev. Phys. Chem.* 41 (1990) 775. and references therein.
- [19] M.M. Biener, J. Biener, R. Schalek, C.M. Friend, *Surf. Sci.* 594 (2005) 221.
- [20] D.V. Potapenko, J.M. Horn, R.J. Beuhler, Z. Song, M.G. White, *Surf. Sci.* 574 (2005) 244.
- [21] J.A. Rodriguez, M. Kuhn, *Surf. Sci. Lett.* 330 (1995) L657.
- [22] D.B. Daño, M. Kuchowicz, R. Szukiewicz, J. Kołaczekiewicz, *Surf. Sci.* 600 (2006) 2258.
- [23] L. Óvári, J. Kiss, *Vacuum* 80 (2005) 204.
- [24] L. Óvári, A.P. Farkas, J. Kiss, F. Solymosi, *Surf. Sci.* 566 (2004) 1082.
- [25] L. Óvári, A.P. Farkas, J. Kiss, F. Solymosi, *J. Phys. Chem. B* 109 (2005) 4638.
- [26] L. Óvári, J. Kiss, *Appl. Surf. Sci.* 252 (2006) 8624.
- [27] M. Oku, H. Matsuta, K. Wagatsuma, Y. Waseda, S. Kohiki, *J. Electron Spectrosc. Relat. Phenom.* 105 (1999) 211.
- [28] A.E. Bocquet, T. Mizokawa, K. Morikawa, A. Fujimori, S.R. Barman, K. Maiti, D.D. Sarma, Y. Tokura, M. Onoda, *Phys. Rev. B* 53 (1996) 1161.
- [29] S. Bartkowski, M. Neumann, E.Z. Kurmaev, V.V. Fedorenko, S.N. Shamin, V.M. Cherkashenko, S.N. Nemnonov, A. Winiarski, *Phys. Rev. B* 56 (1997) 10656.
- [30] A. Berkó, O. Hakkel, J. Szökő, F. Solymosi, *Surf. Sci.* 507 (2002) 643.
- [31] A. Berkó, A. Magony, J. Szökő, *Langmuir* 21 (2005) 4562.
- [32] A. Berkó, I. Ulrych, K.C. Prince, *J. Phys. Chem. B* 102 (1998) 3379.
- [33] G.B. Hoflund, H.-Y. Yin, A.L. Grogan Jr., D.A. Asbury, H. Yoneyama, O. Ikeda, H. Tamura, *Langmuir* 4 (1988) 346.
- [34] J.-M. Pan, B.L. Maschhoff, U. Diebold, T.E. Madey, *J. Vac. Sci. Technol. A* 10 (1992) 2470.
- [35] K. Luo, T. P. St. Clair, X. Lai, D.W. Goodman, *J. Phys. Chem. B* 104 (2000) 3050.
- [36] S.C. Parker, A.W. Grant, V.A. Bondzie, C.T. Campbell, *Surf. Sci.* 441 (1999) 10.
- [37] M.A. Henderson, *Surf. Sci.* 419 (1999) 174.
- [38] W.S. Oh, C. Xu, D.Y. Kim, D.W. Goodman, *Vac. Sci. Technol. A* 15 (1997) 1710.
- [39] T. Sasaki, Y. Goto, R. Tero, K. Fukui, Y. Iwasawa, *Surf. Sci.* 502–503 (2002) 136.
- [40] A.M. Molenbroek, J.K. Norskov, B.S. Clausen, *J. Phys. Chem. B* 105 (2001) 5450.
- [41] J.H. Scofield, *J. Electron Spectrosc. Relat. Phenom.* 8 (1976) 129.
- [42] S. Tanuma, C.J. Powell, D.R. Penn, *Surf. Interface Anal.* 21 (1994) 165.